Strategies to break linear scaling relationships

Javier Pérez-Ramírez [1] and Núria López [2]

The search for new catalytic materials has relied on highly time- and human- resource-consuming procedures. The appearance of theoretical methods that employ density functional theory coupled to kinetic models has allowed the rational understanding of activity volcano plots and selectivity abrupt profiles that resemble cliffs. However, these methodologies present several drawbacks as the optimization is confined to a family of materials, typically metals, and not applied to the overall phase and compositional space, therefore the maximum activity might not be sufficient for practical applications. Volcanos emerge from the symmetry between the adsorption energies of different intermediates on the catalyst, and thus circumventing these dependencies is crucial to identify better catalytic materials. Here we present a revision of the advances in the field that indicate that complexity in the materials is key to identifying alternative paths and thus overcome the drawbacks of scaling relationships.

The not-too-strong, not-too-weak bonding of key intermediates marks the sweet spot fingerprint of optimal catalytic materials. This principle was introduced first by Sabatier, who showed that the light-off temperature of catalysed reactions displayed a volcano shape as a function of formation energies[1,2]. Since then, theoretical approaches to rational catalytic design have been based on identifying the activity of volcanoes and how they depend on a few, descriptors, typically the binding energies of (one or two) intermediates[3,4]. With the appearance of the density functional theory (DFT) and wide-spread access to computers, simulations have been established as one of the pillars in understanding and predicting catalysis. Nowadays, it is possible to implement robust DFT techniques in computational codes, providing detailed electronic structure, thermodynamic and kinetic parameters[5] of increasingly complex reaction networks. Therefore, computationally derived volcano plots have become the gold standard in catalyst design[6]. Volcanos provide a systematic way for catalytic optimization by finely tuning the adsorption energies or through dynamic operation[7], and have proven to be a powerful tool for assessing alloy composition[8], size[9], metal/oxide interfaces[10], pH dependence[11] and have even been reported in homogeneous catalysts[12]. The same principles can be used in electrocatalysis once the potential and pH terms are introduced, and it is likely to appear in photochemistry, although this has not been demonstrated yet.

However, there is an increasing pressure to go beyond the top of these volcanoes[13–15]. There are several reasons behind this need. It is well known that the maximum of the observed rate provides the limit for the activity, and this might be insufficient for the practical application of catalytic technologies[16]. In addition, descriptors are typically energies, and thermodynamics for intermediates cumbersome to obtain experimentally. Moreover, addressing selective processes through volcanoes is not straightforward as several paths need to be investigated with similar accuracy, and the respective volcanoes need to be superimposed[17]. As for the practical aspects, the identified maximum does not provide a synthetic route[18] towards the desired composition. Finally, some false negatives (outliers) might appear as the real phase space is much bigger than a single catalyst family. In summary, the concept of volcano is practical for activity although addresses selectivity and stability aspects poorly. The latter have been solved by applying filters, for instance to assess that the active phase can exist under reaction conditions. Volcanos are not so useful for full-phase space discovery in their present formulation, but they are very convenient for catalyst optimization within a family of compounds, for example, alloys and bimetallics. In the following, we address the different approximations that have been employed in the literature to alleviate the limitations of the volcanoes by increasing the complexity of materials and the chemical variability. To this end, we first describe the appearance of the linear scaling relationships (LSRs) and how these are transferred into the volcano and cliff shapes once microkinetic balances are considered and then provide a perspective on the strategies in the literature to alter LSRs by increasing complexity.

The origin of volcanos and cliffs

To improve catalytic performance beyond the volcanos it is necessary to understand why they appear. The procedure is exemplified in Fig. 1, where the particular model employed comprises a selective process (A+1/2B→P) and a side path (A→Q), the models for which can be accessed from ref. [19]. The standard procedure is as follows: the detailed reaction network is mapped carefully for at least one catalytic compound and the corresponding energies are calculated by DFT, then a microkinetic model that wraps all the elementary steps is developed. In a complex reaction with multiple intermediates, it turns out that the bond order conservation theory and the electron counting rules imply that the energies of intermediates are linked one to another in a linear manner (tLSRs[20], Fig. 1a). This is particularly applicable to metals for which the smoothness of the electron cloud helps address density fluctuations better. For metals, the local coordination number can also generate LSR and cLSR[21]. Brønsted–Evans–Polanyi, as well as several others, found that the kinetic terms depend linearly on thermodynamic parameters, and thus the activation barriers can be traced back to the energy of one or more intermediates in a linear form (kinetic linear scaling relationships, kLSRs), Fig. 1b[22]. These kLSRs are also known in the literature as linear free energy relationships (LFER) or Bronsted–Evans–Polanyi (BEP) relationships. When the dependencies encoded in the LSRs are introduced in the rate expression, activity shows the volcano shape as a function of specific adsorption energies for key intermediates, as seen in Fig. 1c, with the highest activity marked by an asterisk (see Fig. 1e for a particular cut in a monodimensional space). Therefore, a strong adsorption implies high coverage and surface poisoning, and a weak adsorption entails very low coverage and thus low rate; in both cases

[1]Institute for Chemical and Bioengineering, ETH Zurich, Zurich, Switzerland. [2]Institute of Chemical Research of Catalonia, The Barcelona Institute of Science and Technology, Tarragona, Spain. e-mail: jpr@chem.ethz.ch; nlopez@iciq.es

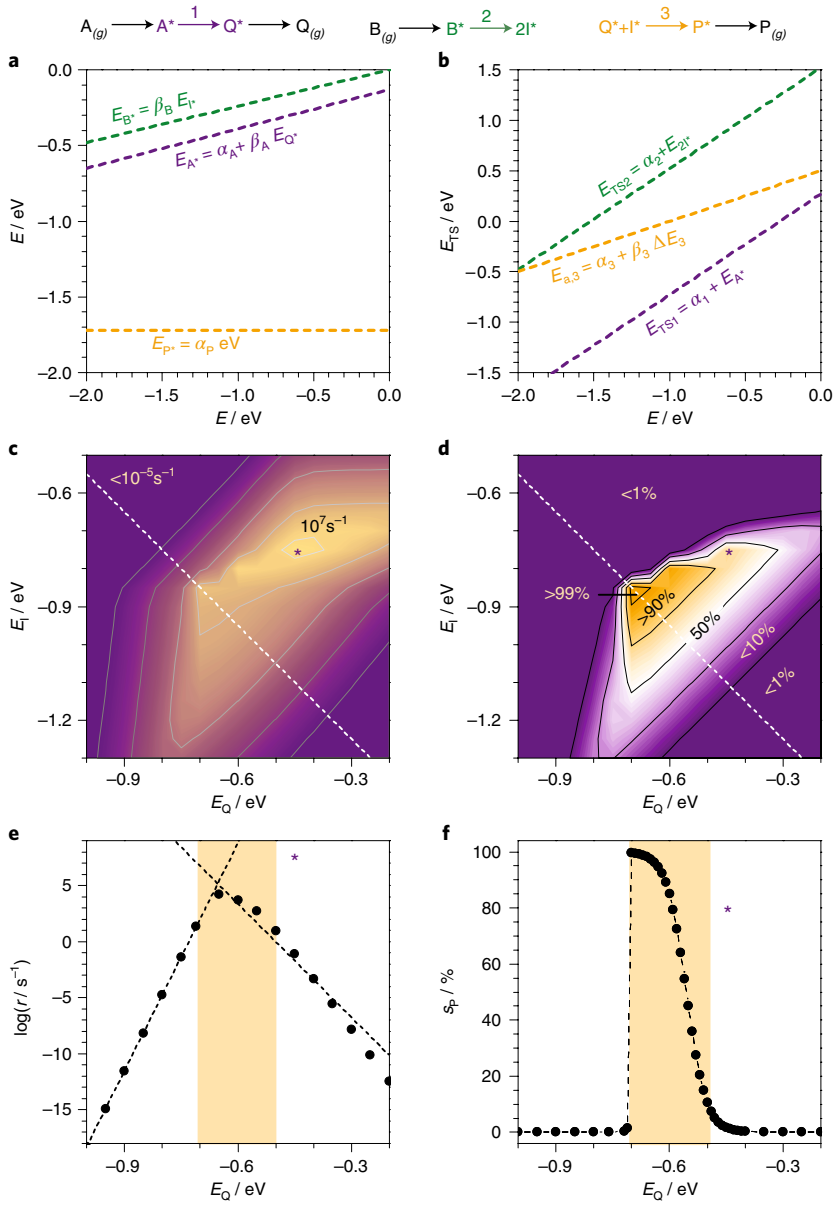

Fig. 1 | Competitive reaction network to convert A and B into P and Q as desired and undesired products, respectively. a,**b**, Thermodynamic and kinetic linear scaling relationships (tLSRs and kLSRs, respectively. **c**,**d**, Activity and selectivity volcanos as a function of the adsorption energy of **Q** and **I**. An asterisk indicates the condition that maximizes the production of **P** although with a moderate selectivity (~50%). An optimization strategy is presented as a dashed white line. **e**,**f**, One-dimensional activity volcano and selectivity cliff (the cuts were done along the dotted lines marked in c,d. The selectivity has a cliff where **Q** binds more strongly than **I** and thus poisons the surface. Models are from ref. [19], Zenodo.

the reaction is hindered. Contrarily to the smoothness found for activity volcanoes, selectivity relies on the difference between two competing steps, and these very small energy differences generate discontinuities in the behaviour, acting as an on/off switch and resulting in much more abrupt profiles, as seen in Fig. 1f. The reason behind this is that very small energy differences, as small as <0.10 eV at normal conditions, might turn a selective process into an unselective one[23], thus approaching the limit of DFT accuracy energy. If the kLSRs for the desired and undesired products have different slopes when written as a function of the energy of the key intermediate, as seen in Fig. 1b, then cliffs emerge in the volcano plots (see Fig. 1d, f), and actually the point with the highest selectivity might depart from the point with the best activity.

Therefore, reaching activities that are higher than those marked by the volcano limitations implies breaking the symmetry rules (dependencies) imposed by the LSRs. This can only be done by including alternative energy forms or increasing the complexity of the catalyst.

Circumventing linear scaling relationships

In 2015, Vojvodic and Nørskov listed several potential ways of breaking or circumventing LSRs[24]. Following the traditional analysis, geometric and electronic terms, as well as intrinsic or extrinsic effects, were taken as orthogonal directions for development. Disentangling the geometric and electronic effects is difficult, some suggestions have been put forward[25]. The activity has been very large in the field and in Fig. 2 we present the already identified ways to elude the LSRs for which examples exist.

The simplest way to circumvent LSRs is through a pure geometrical effect. Strain has been used in this context[26], as the binding

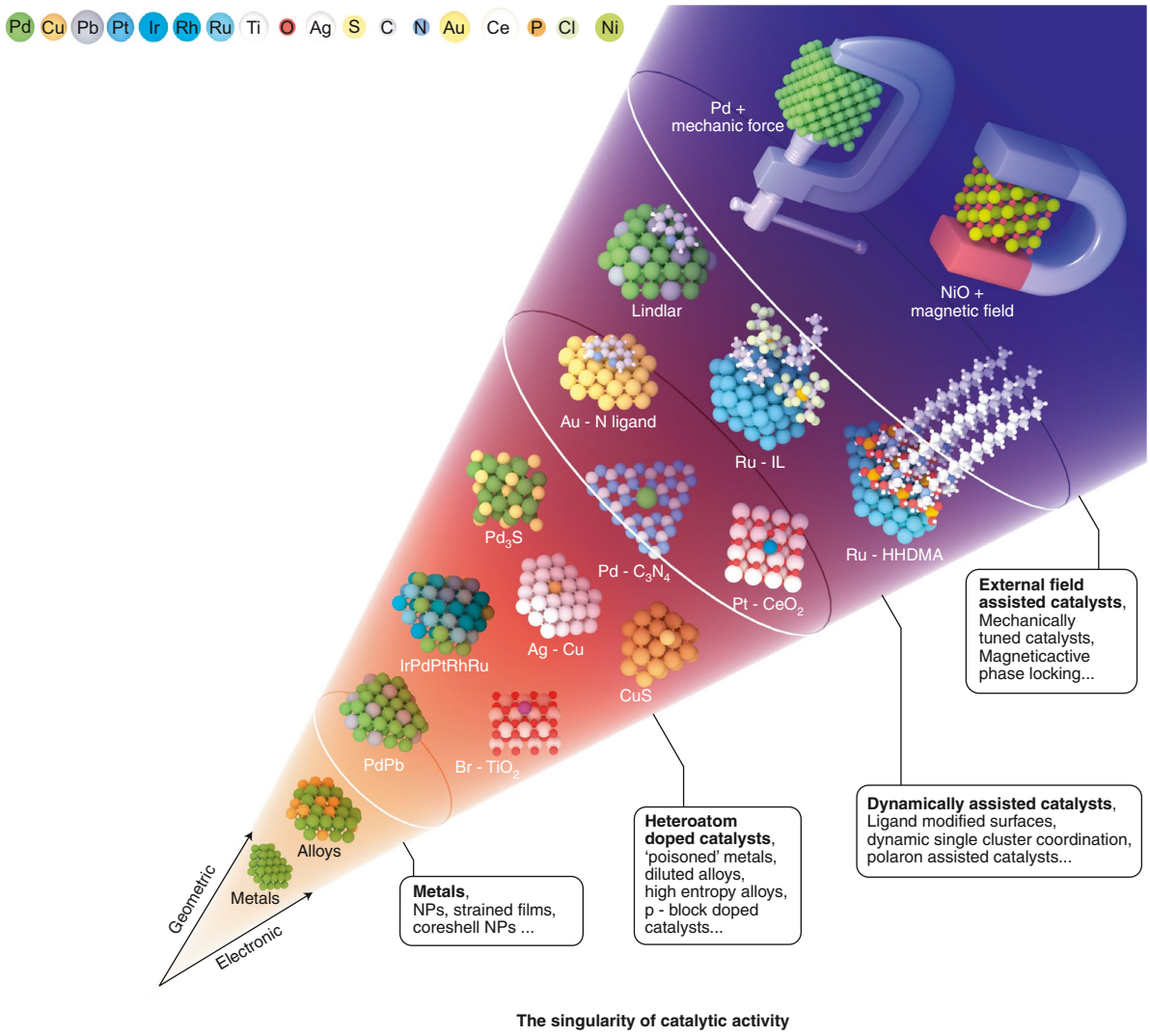

Fig. 2 | The cone timeline of breaking linear-scaling relationships strategies. Structures are placed according to their mostly electronic or mostly geometric contributions. The identified rules can be described in terms of complexity (diagonal timeline). The lowest design level corresponds to metal-only systems and simple alloys and the changes induced by strain[26] or coordination. The second level is formed by doped systems: metal-in-metal single atoms[27], high entropy alloys[39], self-doped semiconductors[41], p-doped systems[53]. The third complexity level encompasses ligand modified systems[42], organometallic systems[59], single atoms in carbon matrixes[30] and their dynamic electronic and geometric effects[56]. The highest level corresponds to the introduction of external forces[62–64], such as light, mechanic or magnetic forces.

energy of different species may depend on the geometric perturbation in different directions. Alternatively, ensemble control requires the identification of the minimum site to perform the desired reaction and space, and to resolve it in a controlled manner. Actually, this effect is really acting on the selectivity control, particularly as some reactions might require larger ensembles than others. The way to access this control is by alloying with inert species (Au, ref. [27]); adsorbing molecular fragments (selectivity modulators), as in the Lindlar catalyst[28] or NanoSelect[29]. This method has been used recently in single-atom catalysts[30,31], and *p*-block modified phases like PdS_x active materials[32]. All these changes also modify the electronic structure (and even bifunctional mechanisms appear with reactants adsorbed in different sites, such as PdS_x) but the ensemble contribution is the most obvious by far. The best example can be found for the hydrogenation of alkynes: while the desired path requires very small ensembles (3–4 atoms), the parasitic reaction C–C bond formation demands more than six atoms. Therefore, limiting the ensemble is a selectivity enhancer, and this is achieved by breaking the LSRs for the C–C bond formation. This has been found by sulfiding supported Pd nanoparticles under mild conditions, which results in facet control by kinetic terms[33]. Therefore, the nuclearity control when using small clusters can fine-tune the selectivity[34–36]. Similar concepts have been employed in metal-only single-atom catalysts, where the resistance towards coking[37,38] and the long-term stability of the catalyst are due to the suppression of the side decomposition path that does not scale any longer with the intermediates. High-entropy alloys are an alternative, as the continuous nature of adsorption is an effective way to modulate reactivity[39]. Notice, however, that metal in metal systems (without a phase change) can only provide solutions to the selectivity cliffs (and in doing so improve the yield and the long-term stability) but not to the underlying activity, as the density anisotropies are very small in these materials.

A fully electronic effect was found in the Br version of the Deacon reaction ($HBr + \frac{1}{2}O_2 \rightarrow Br_2 + H_2O$) on oxides of the rutile family, most of them with a metallic character. The reaction encompasses surface oxidation, the adsorption of the acid, the halogen evolution, hydroxyl recombination and, finally, water elimination. When

considered in this order, the reaction is found to be unfeasible on TiO_2 rutile, a semiconductor that cannot adsorb O_2 (ref. [40]). However, the order of the competing adsorbing reactions is arbitrary. For example, when starting the reaction by HBr adsorption, the system self-dopes and leads to an effective catalyst by breaking the rules between O and Br adsorption on rutiles[41]. An important conclusion is that, besides geometry, the particular electronic structure for the material is crucial, and results from metal-like materials cannot be extrapolated to semiconductors.

Electronic and geometric terms are generally not so easy to separate. The addition of external elements, like ligands to metal surfaces, can also provide other electronic effects. For instance, electrostatics and hydrogen bonds are found to rearrange intermediates in the direct hydrogenation of O_2 (towards H_2O_2) or for nitrogen to ammonia from planarly bonded OOH or NNH (prone to dissociation) towards standing species where the lack of bonds to the surface prevent effective dissociation[42,43]. The LSR for the planar and vertical configurations is thus different when electric fields, ligands and ionic liquids exist[42,43]. Again, in the first case, the selectivity switch goes on top of the activity control.

In all of the previous cases, the changes mostly affected the viability of the reaction network and not in the particular nature of the species involved. However, this is one of the most effective ways to circumvent LSRs. For instance, hydrogenation on metal surfaces takes place via the Horiuti–Polanyi mechanism[44], that is, by splitting H_2 into two H atoms and transferring them sequentially, although other ways are also possible. On gold-decorated nanoparticles with ligands containing H_2 bonds, the ligands play an active role and induce the dissociation as hydride-proton[45]. On the other hand, if the ligand contains C=O terminations, then hydrogenation occurs through a concerted step[46] transfer hydrogenation. In both cases, the kLSR breaks because the transition states are different from those of the regular surface. This is also the case of the single Pd atoms stabilized on carbon nitride in which the scaffold acts as a ligand[30]. Moreover, the presence of polarity between cations and anions in oxides leads to a heterolytic dissociation path[47].

Hydrogen molecules can still be separated as two protons and two electrons, which gives rise to two alternative hydrogenation mechanisms. For instance, catalyst acidity is fundamental to the conversion of acidic biomass molecules. Ru nanoparticles decorated by surfactants (HHDMA) split H_2 into protons and electrons. The metal–ligand interface is so strongly acidic[48] that it can protonate levulate, the most common form in a water-based solution of levulinic acid, and thus enable the transformation to γ-valerolactone, one of the twelve most demanded chemicals derived from biomass. This protonation overrules the reaction mechanism of levulate on Ru, which is rather inefficient. pH effects can also tune the catalytic route and change the active volcano[49]. Very small decorated Pt nanoparticles can also store electrons at high potentials, which can be used for the selective reduction of nitrobenzene to aniline. For such systems, the interface electric field, coupled to the size of the nanoparticles (around 1.2–1.5 nm), creates the driving force for changing the active species from H atoms on the surface into high potential electrons[50]. The decoration with chiral substrates can also alter the reactivity and displace the rate-determining reaction to be spin controlled, as has been found for the oxygen evolution reaction on chiral-decorated iron oxides. This appears to be consequence of the spin-polarized nature of O_2 that can be only achieved when the surface is ferromagnetically aligned[51].

Cooperative effects can also help reducing inefficiencies in reaction paths. Simple coverage effects can be deemed responsible for better performance due to rearrangements that make competing kLSRs more chemoselective towards the desired product at higher coverages[52]. Alternatively, impurities such as sulfur can preferentially trap CO_2 on Cu in electrochemical environments. The tethering[53] of the key species allows blocking of the unselective path for geometric reasons. The ultimate consequence is a complete change in selectivity as the decorated system produces formate instead of CO, as would occur on Cu, producing formate instead. Active ligands can be employed as reactant relays[54] in homogeneous electrocatalysis; this effect could be equivalent to Mars-van-Krevelen processes in heterogeneous catalysis, and thus does not follow surface LSRs. Bifunctional mechanisms also belong to this class, since a part of the path can occur at one centre while a second conversion takes place on a different area of the catalyst[55].

Dynamics can offer a way to overcome LSRs, however, the control at the nanoscale is not evident from our present tools. For instance, the fluxionality of small nanoparticles can interconnect different geometric configurations with different properties for the adsorption of intermediates, thus breaking the rules by adapting the coordination in each case[56]. Ligands can also dynamically cover parts of the surface, leading to short-lived highly selective active sites[57]. This effect can be amplified and modified when a support exists[58]. The effect is particularly important in homogeneous catalysis, and in this way in molecular systems LSR can be disrupted through geometric strain, which influences the electronic properties and decouples reaction steps[59]. Alternatively, the electronic dynamics can also contribute to differential reactivity, as has been found for CO oxidation on dynamic charge transfer systems, such as single-atom platinum on CeO_2 where more than one electronic state is available, allowing a low-temperature reaction path[60].

Finally, the use of other external forces can break LSRs[61]. Recently, mechanochemistry has emerged as a way to enhance the catalytic response, and in this case reactions are carried out with the minimum solvent and by grinding the solid reactants[62]. Plasmonic metal nanoparticles can also drive new transformations effectively. The incoming electromagnetic radiation in the form of light concentrates in the form of plasmons and therefore results new activity rules[63]. Similarly, the oxygen evolution reaction on antiferromagnets at high pH has been found to be enhanced by magnetic effects due to spin-control in the reaction[64]. All these processes differ from standard temperature control and different linear scaling can be envisaged.

Conclusions

In summary, much progress has been made in alternative ways to circumvent linear scaling relationships, particularly those affecting selectivity, as blocking the lateral paths improves both activity and stability. However, a general overall optimization including unchartered territories is not yet possible, partially because of the lack of fundamental understanding of the properties of complex electronic structure materials (https://materialsproject.org/) and the very limited atomistic investigations on complex multiphase materials or interfaces. Understanding complexity will require the combination of the descriptor strategies with high-throughput experimentation approaches, as well as detailed synthetic control and characterization tools to unveil alternative catalytic routes that circumvent the present linear-scaling relationships.

Code Availability

The model systems for Fig. 1 can be retrieved from ref. [19].

Received: 25 July 2019; Accepted: 27 September 2019;
Published online: 28 October 2019

References

1. P. Sabatier. *La Catalyse en Chimie Organique* (Librarie Polytechnique, Paris, 1913).
2. Balandin, A. Modern State of the Multiplet Theory of Heterogeneous Catalysis 1. *Adv. Catal. Rel. Subj.* **19**, 1 (1969).
3. Nørskov, J. K., Bligaard, T., Rossmeisl, J. & Christensen, C. H. Towards the computational design of solid catalysts. *Nat. Chem.* **1**, 37–46 (2009).
4. Nørskov, J. K., Studt, F., Abild-Pedersen, F., Bligaard, T. *Fundamental concepts in heterogeneous catalysis* (Wiley, 2014).

5. Lejaeghere, K. et al. Reproducibility in density functional theory calculations of solids. *Science* **351**, aad3000 (2016).
6. Medford, A. J. et al. From the Sabatier principle to a predictive theory of transition-metal heterogeneous catalysis. *J. Catal.* **328**, 36–42 (2015).
7. Ardagh, M. A., Abdelrahman, O. A. & Dauenhauer, P. J. Principles of dynamic heterogeneous catalysis: surface resonance and turnover frequency response. *ACS Catal.* **9**, 6929–6937 (2019).
8. Greeley, J. et al. Alloys of platinum and early transition metals as oxygen reduction electrocatalysts. *Nat. Chem* **1**, 552–556 (2009).
9. Vilè, G. et al. Silver nanoparticles for olefin production: new insights into the mechanistic description of propyne hydrogenation. *ChemCatChem* **5**, 3750–3759 (2013).
10. Choksi, T., Majumdar, P. & Greeley, J. P. Electrostatic origins of linear scaling relationships at bifunctional metal/oxide interfaces: a case study of Au nanoparticles on doped MgO substrates. *Angew. Chem. Int. Ed.* **57**, 15410–15414 (2018).
11. Koper, M. T. M. Volcano activity relationships for proton-coupled electron transfer reactions in electrocatalysis. *Top. Catal.* **58**, 18–20 (2015).
12. Busch, M., Wodrich, M. D. & Corminboeuf, C. Linear scaling relationships and volcano plots in homogeneous catalysis–revisiting the Suzuki reaction. *Chem. Sci.* **6**, 6754–6761 (2015).
13. Busch, M. et al. Beyond the top of the volcano?–A unified approach to electrocatalytic oxygen reduction and oxygen evolution. *Nano Energy* **29**, 126–135 (2016).
14. Halck, N. B., Petrykin, V., Krtil, P. & Rossmeisl, J. Beyond the volcano limitations in electrocatalysis–oxygen evolution reaction. *Phys. Chem. Chem. Phys.* **16**, 13682–13688 (2014).
15. Li, Y. & Sun, Q. Recent advances in breaking scaling relations for effective electrochemical conversion of CO_2. *Adv. Ener. Mat.* **6**, 1600463 (2016).
16. Szécsényi, Á. et al. Breaking linear scaling relationships with secondary interactions in confined space: a case study of methane oxidation by Fe/ZSM-5 zeolite. *ACS Catal.* **9**, 9276–9284 (2019).
17. Cao, A. et al. Mechanistic insights into the synthesis of higher alcohols from syngas on CuCo alloys. *ACS Catal.* **8**, 10148–10155 (2018).
18. Kanady, J. S. et al. Synthesis of Pt_3Y and other early–late intermetallic nanoparticles by way of a molten reducing agent. *J. Am. Chem. Soc.* **139**, 5672–5675 (2017).
19. García-Muelas, R. Minimalistic microkinetic model with volcanoes and cliffs. *Zenodo* https://doi.org/10.5281/zenodo.3338280 (2019).
20. Abild-Pedersen, F. et al. Scaling properties of adsorption energies for hydrogen-containing molecules on transition-metal surfaces. *Phys. Rev. Lett.* **99**, 016105 (2007).
21. Calle-Vallejo, F. et al. Introducing structural sensitivity into adsorption-energy scaling relations by means of coordination numbers. *Nat. Chem.* **7**, 403–410 (2015).
22. Bligaard, T. et al. The Bronsted–Evans–Polanyi relation and the volcano curve in heterogeneous catalysis. *J. Catal.* **224**, 206–217 (2004).
23. Medford, A. J. et al. Activity and selectivity trends in synthesis gas conversion to higher alcohols. *Top. Catal.* **57**, 135–142 (2014).
24. Vojvodic, A. & Nørskov, J. K. New design paradigm for heterogeneous catalysts. *Natl. Sci. Rev.* **2**, 140–149 (2015).
25. Wang, H. et al. Disentangling the size-dependent geometric and electronic effects of palladium nanocatalysts beyond selectivity. *Sci. Adv.* **5**, eaat6413 (2019).
26. Khorshidi, A., Violet, J., Hashemi, J. & Peterson, A. A. How strain can break the scaling relations of catalysis. *Nat. Catal.* **1**, 263–268 (2018).
27. Kyriakou, G. et al. Isolated metal atom geometries as a strategy for selective heterogeneous hydrogenations. *Science* **335**, 1209–1212 (2015).
28. Lindlar, H. Ein neuer Katalysator für selektive Hydrierungen. *Helv. Chim. Acta* **35**, 446 (1952).
29. Vilè, G. et al. From the Lindlar catalyst to supported ligand modified palladium nanoparticles: selectivity patterns and accessibility constraints in the continuous flow three phase hydrogenation of acetylenic compounds. *Chem. Eur. J.* **20**, 5926–5937 (2014).
30. Vilè, G. et al. A stable single site palladium catalyst for hydrogenations. *Angew. Chem. Int. Ed.* **54**, 11265–11269 (2015).
31. Darby, M. T., Stamatakis, M., Michaelides, A. & Sykes, E. C. H. Lonely atoms with special gifts: breaking linear scaling relationships in heterogeneous catalysis with single-atom alloys. *J. Phys. Chem. Lett.* **9**, 5636–5646 (2018).
32. McKenna, F.-M. & Anderson, J. A. Selectivity enhancement in acetylene hydrogenation over diphenyl sulphide-modified Pd/TiO_2 catalysts. *J. Catal.* **281**, 231–240 (2011).
33. Albani, D. Selective ensembles in supported palladium sulfide nanoparticles for alkyne semi-hydrogenation. *Nat. Comm.* **9**, 2634 (2018).
34. Vajda, S. et al. Subnanometre platinum clusters as highly active and selective catalysts for the oxidative dehydrogenation of propane. *Nat. Mat.* **8**, 213–216 (2009).
35. Voroyeva, E. et al. Atom-by-atom resolution of structure–function relations over low-nuclearity metal catalysts. *Angew. Chem. Int. Ed.* **58**, 8724 (2019).
36. Frei, M. S. et al. Atomic-scale engineering of indium oxide promotion by palladium for methanol production via CO_2 hydrogenation. *Nat. Comm.* **10**, 3377 (2019).
37. Marcinkowski, M. D. et al. Pt/Cu single-atom alloys as coke-resistant catalysts for efficient C–H activation. *Nat. Chem.* **10**, 325–332 (2018).
38. Sun, D. et al. Breaking the scaling relationship via thermally stable Pt/Cu single atom alloys for catalytic dehydrogenation. *Nat. Comm.* **9**, 4454 (2018).
39. Batchelor, T. A. A. et al. High-entropy alloys as a discovery platform for electrocatalysis. *Joule* **3**, 834–845 (2019).
40. Studt, F. Volcano relation for the Deacon process over transition metal oxides. *ChemCatChem* **2**, 98–102 (2010).
41. Moser, M. et al. The virtue of defects: stable bromine production by catalytic oxidation of hydrogen bromide on titanium oxide. *Angew. Chem. Int. Ed.* **53**, 8628–8633 (2014).
42. Lari, G. M. et al. Hybrid palladium nanoparticles for direct hydrogen peroxide synthesis: the key role of the ligand. *Angew. Chem. Int. Ed.* **129**, 1801–1805 (2014).
43. Ortuño, M. A. Selective electrochemical nitrogen reduction driven by hydrogen bond interactions at metal–ionic liquid interfaces. *J. Phys. Chem. Lett.* **10**, 513–517 (2019).
44. Horiuti, I. & Polanyi, M. Exchange reactions of hydrogen on metallic catalysts. *J. Chem. Soc. Faraday Trans.* **30**, 1164–1172 (1934).
45. Fiorio, J. L., López, N. & Rossi, L. M. Gold–ligand-catalyzed selective hydrogenation of alkynes into cis-alkenes via H_2 heterolytic activation by frustrated lewis pairs. *ACS Catal.* **7**, 2973–2980 (2017).
46. Almora-Barrios, N., Cano, I., van Leeuwen, P. W. N. M. & López, N. Concerted chemoselective hydrogenation of acrolein on secondary phosphine oxide decorated gold nanoparticles. *ACS Catal.* **7**, 3949–3954 (2017).
47. García-Melchor, M. & López, N. Homolytic products from heterolytic paths in H_2 dissociation on metal oxides: the example of CeO_2. *J. Phys. Chem. C.* **118**, 10921–10926 (2014).
48. Albani, D. et al. Interfacial acidity in ligand-modified ruthenium nanoparticles boosts the hydrogenation of levulinic acid to gamma-valerolactone. *Green. Chem.* **19**, 2361–2370 (2017).
49. Wang, Y.-H. et al. Brønsted acid scaling relationships enable control over product selectivity from O_2 reduction with a mononuclear cobalt porphyrin catalyst. *ACS Cent. Sci.* **5**, 1024–1034 (2019).
50. Almora-Barrios, N. et al. Electrochemical effects at surfactant–platinum nanoparticle interfaces boost catalytic performance. *ChemCatChem* **9**, 604–609 (2017).
51. Zhang, W. et al. Enhanced electrochemical water splitting with chiral molecule-coated Fe_3O_4 nanoparticles. *ACS Energy Lett.* **3**, 2308–2313 (2018).
52. Tuokko, S., Pihko, P. M. & Honkala, K. First principles calculations for hydrogenation of acrolein on Pd and Pt: chemoselectivity depends on steric effects on the surface. *Angew. Chem. Int. Ed.* **128**, 1702–1706 (2016).
53. García-Muelas, R. et al. Origin of the selective electroreduction of carbon dioxide to formate by chalcogen modified copper. *J. Phys. Chem. Lett.* **9**, 7153–7159 (2018).
54. Zhan, S., De Gracia Triviño, J. A. & Ahlquist, M. S. G. The carboxylate ligand as an oxide relay in catalytic water oxidation. *J. Am. Chem. Soc.* **141**, 10247–10252 (2019).
55. Zhang, B. et al. Homogeneously dispersed multimetal oxygen-evolving catalysts. *Science* **352**, 333–337 (2016).
56. Zandkarimi, B. & Alexandrova, A. N. Dynamics of subnanometer Pt clusters can break the scaling relationships in catalysis. *J. Phys. Chem. Lett.* **10**, 460–467 (2019).
57. Ortuño, M. A. & Lopez, N. Creating cavities at palladium–phosphine interfaces for enhanced selectivity in heterogeneous biomass conversion. *ACS Catal.* **8**, 6138–6145 (2018).
58. Kauppinen, M. M., Korpelin, V., Verma, A. H., Melander, M. M., Honkala, K. Escaping scaling relationships for water dissociation at interfacial sites of zirconia-supported Rh and Pt clusters. Preprint at https://doi.org/10.26434/chemrxiv.9761477.v1 (2019).
59. Gani, T. Z. H. & Kulik, H. J. Understanding and breaking scaling relations in single-site catalysis: methane to methanol conversion by Fe^{IV}═O. *ACS Catal.* **8**, 975–986 (2018).
60. Daelman, N., Capdevila-Cortada, M., López, N. Dynamic charge and oxidation state of Pt/CeO_2 single-atom catalysts. *Nat. Mat.* https://doi.org/10.1038/s41563-019-0444-y (2019).
61. Robertson, J. C., Coote, M. L. & Bissember, A. C. Synthetic applications of light, electricity, mechanical force and flow. *Nat. Rev. Chem.* **3**, 290–304 (2019).
62. James, S. L. et al. Mechanochemistry: opportunities for new and cleaner synthesis. *Chem. Soc. Rev.* **41**, 413–447 (2012).
63. Linic, S., Christopher, P. & Ingram, D. B. Plasmonic-metal nanostructures for efficient conversion of solar to chemical energy. *Nat. Mat.* **10**, 911–321 (2011).
64. Garcés-Pineda, F. et al. Direct magnetic enhancement of electrocatalytic water oxidation in alkaline media. *Nat. Energy* **4**, 519–525 (2019).

Acknowledgements
We would like to thank E. Fako and R. García-Muelas for their assistance with Figs., microkinetic modelling and for critically reading the manuscript.

Competing Interests
The authors declare no competing interests.

Additional information
Correspondence should be addressed to J.P.-R. or N.L.